Case I Coherence Effects

Ultrasonic Attenuation

$$H_{pert} = \lambda\, q\, u_0 e^{i(qx-\omega t)} \sum_{k,k',\sigma,\sigma'} c_{k\sigma}^{+} c_{k'\sigma'}$$

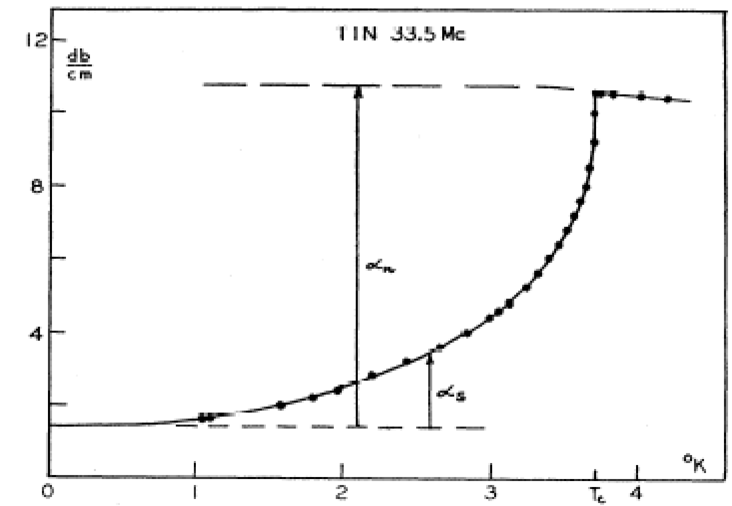

FIG. 1. Measured ultrasonic attenuation of longitudinal waves in a tin single crystal at a frequency of 33.5 Mc/sec.

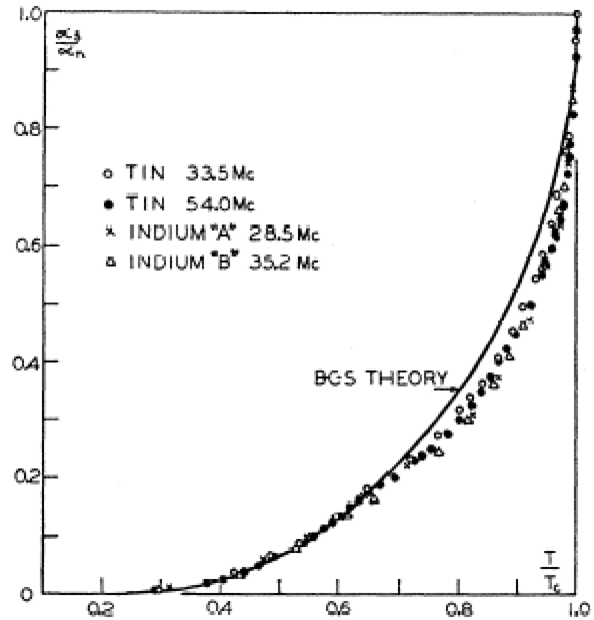

FIG. 2. Measured values of α_s/α_n compared with the theoretical variation of Bardeen, Cooper, and Schrieffer assuming $\epsilon_0(0) = 1.75kT_c$. For tin $T_c = 3.71$ °K and for indium $T_c = 3.40$ °K.

R. W. Morse and H. V. Bohm, Phys. Rev. **108**, 1094 (1957)

Hebel-Slicther Coherence Peak

L. C. Hebel and C. P. Slichter, Phys. Rev. **113**, 1504 (1959).

Case II
Coherence Effects

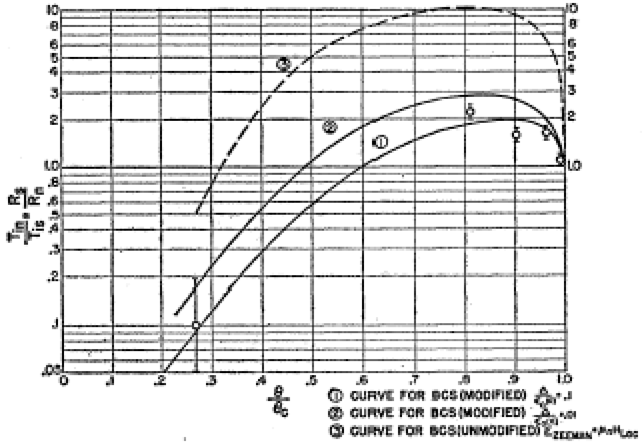

FIG. 3. Relaxation rate in a superconductor, R_s, relative to the zero-field value extrapolated from the normal state, $R_n(0)$, *versus* reduced temperature θ/θ_c. The three theoretical curves using BCS theory are described in the text.

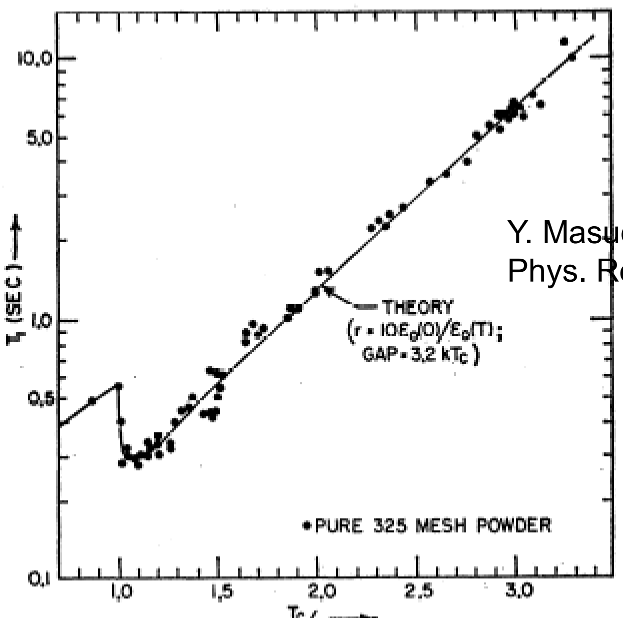

Y. Masuda and A. G. Redfield Phys. Rev. **125**, 159 (1962)

FIG. 2. Measured values of T_1 in the powdered sample. No points were rejected, so that the scatter gives a fairly good idea of the accuracy. T_u was taken to be 1.178°K. The theoretical curve is the same as the solid line of Fig. 5.

FIG. 2. Measured values of T_1 in the powdered sample. No points were rejected, so that the scatter gives a fairly good idea of the accuracy. T_u was taken to be 1.178°K. The theoretical curve is the same as the solid line of Fig. 5.

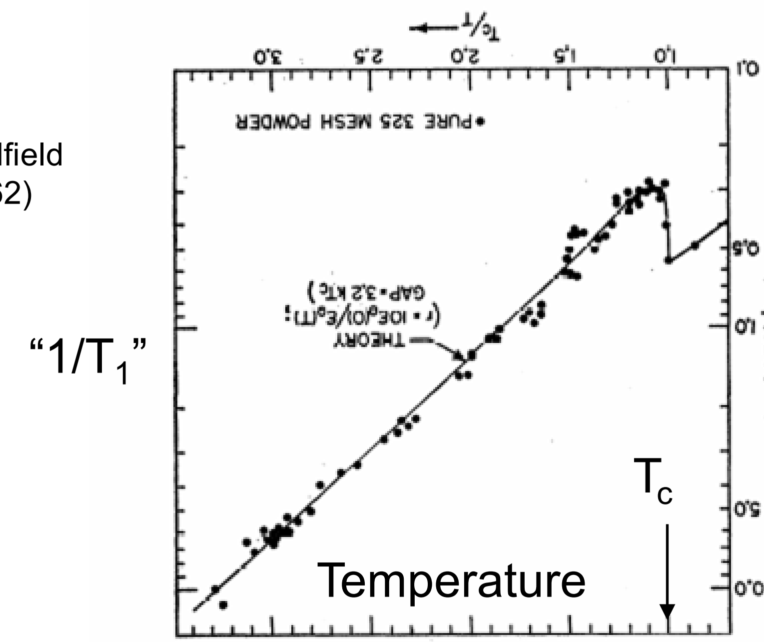

Case II Coherence Effects in σ_1(T)

Nb_3Sn

“BCS Coherence Peak”

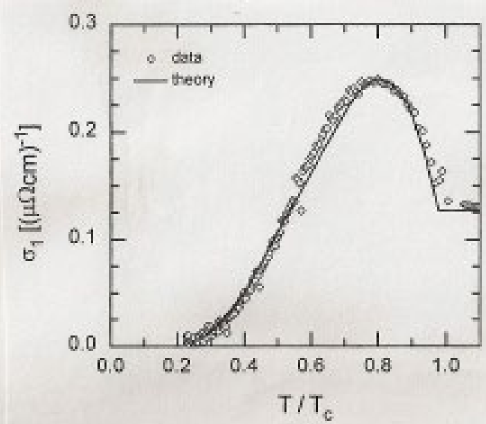

Fig. 2.12. Temperature dependent quasi-particle conductivity $\sigma_1(T)/\sigma_1(T_c)$, deduced from the data at 87 GHz in Fig. 2.10 after subtraction of the residual surface resistance, compared with the expectation from BCS theory for low frequencies [98] (see Fig. 1.7 in Sect. 1.3.2).

Nb_3Sn and Cuprate

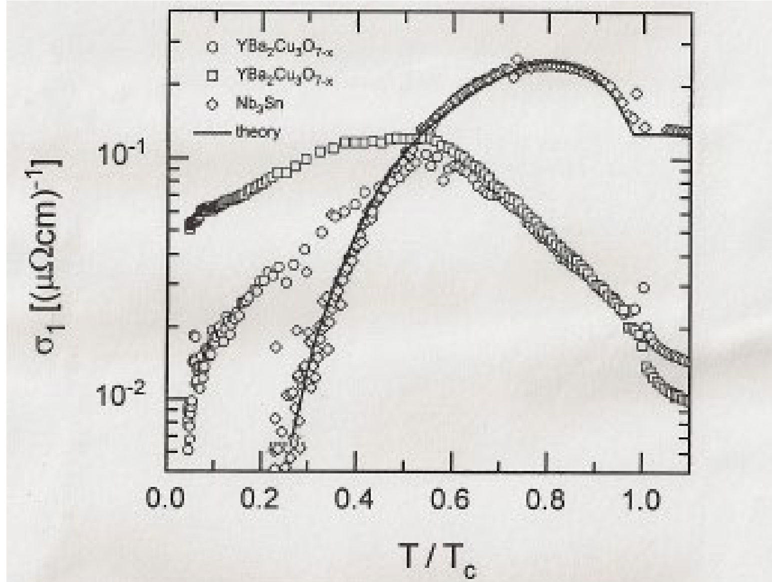

Fig. 2.20. Quasi-particle conductivity $\sigma_1(T)$ versus T/T_c for two epitaxial YBCO films (*circles* and *squares*), and a Nb_3Sn film on sapphire prepared by TVD (Fig. 2.12). Also shown is the low-frequency expectation for the coherence peak at 2% smearing of the energy gap (*solid line*, see Fig. 1.7).

M. Hein, Habilitation Thesis

BCS Coherence Peak in $\sigma_1(T)$

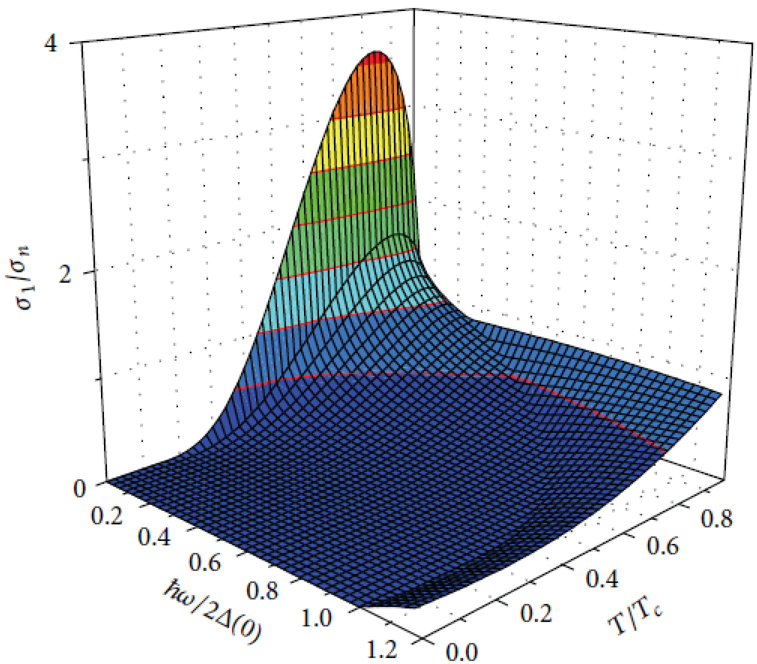

FIGURE 2: Frequency and temperature dependence of the real part of the conductivity σ_1/σ_n calculated according the BCS theory [27, 28] with the ratio of the coherence length to the mean free path $\pi\xi(0)/2\ell = 10$. The pronounced maximum for low frequencies at a temperature slightly below T_c is the coherence peak. The kink at $\hbar\omega = 2\Delta(0)$ corresponds to the superconducting gap that decreases with temperature and vanishes for $T \rightarrow T_c$ (after [29]).

M. Dressel, "Electrodynamics of Metallic Superconductors," Advances in Condensed Matter Physics **2013, 25 (2013).**

The Coherence Peak in $\sigma_1(T,\omega)$ Fades Away as $\hbar\omega \to \Delta$

$$\frac{\alpha_s}{\alpha_n} = \frac{1}{\hbar\omega}\int_{-\infty}^{+\infty} \frac{\left|E(E+\hbar\omega)\mp\Delta^2\right|(f(E)-f(E+\hbar\omega))}{\sqrt{E^2-\Delta^2}\sqrt{(E+\hbar\omega)^2-\Delta^2}}dE$$

Coherence are strongest when $\hbar\omega \ll \Delta$

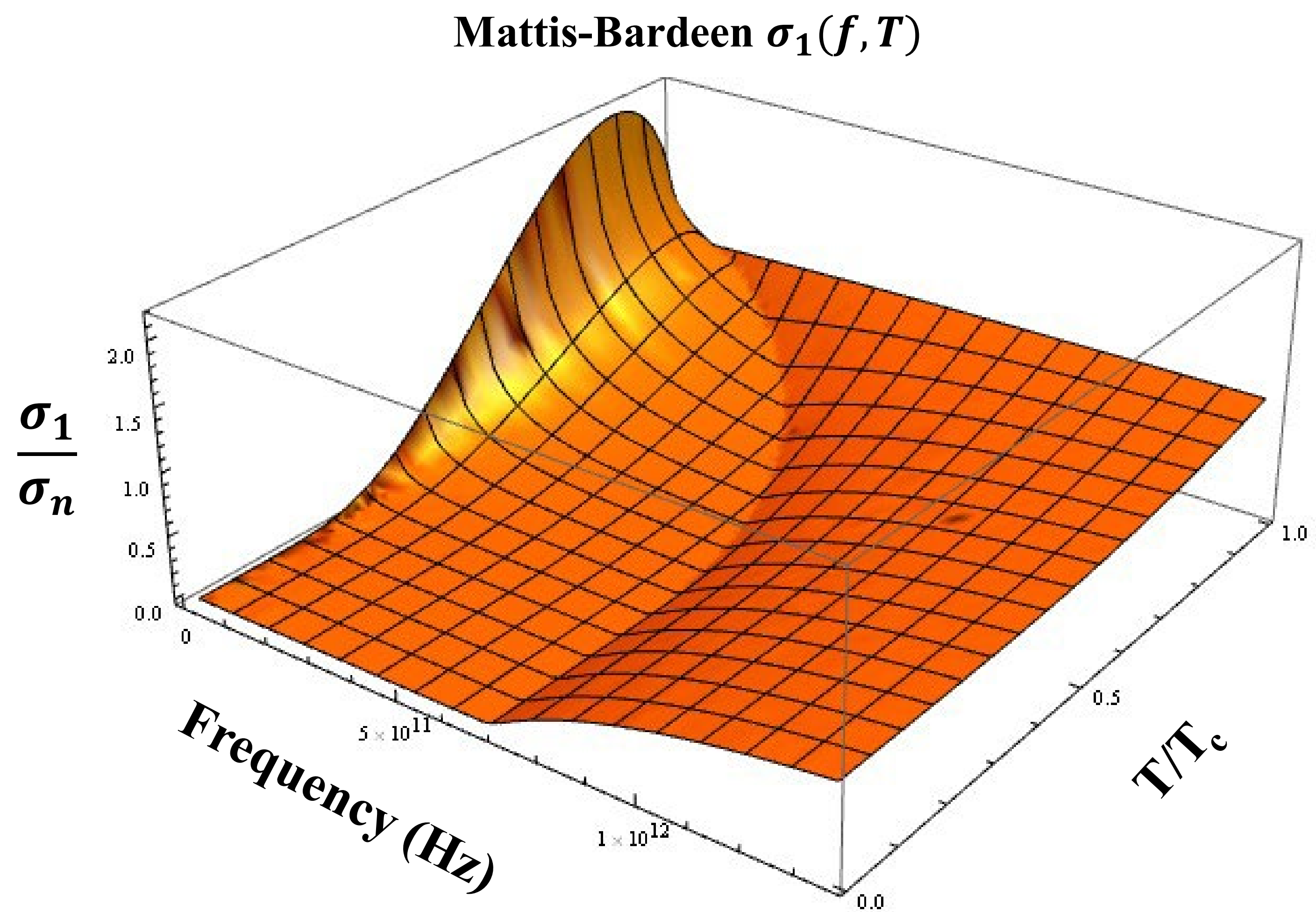

Mattis-Bardeen $\sigma_1(f,T)$
$\frac{\sigma_1}{\sigma_n}$
2.0
1.5
1.0
0.5
0.0
0
5×10^{11}
1×10^{12}
Frequency (Hz)
0.0
0.5
1.0
T/T_c

D. M. Ginsburg and M. Tinkham, Phys. Rev. **118**, 990 (1960)

Case II Coherence Effects

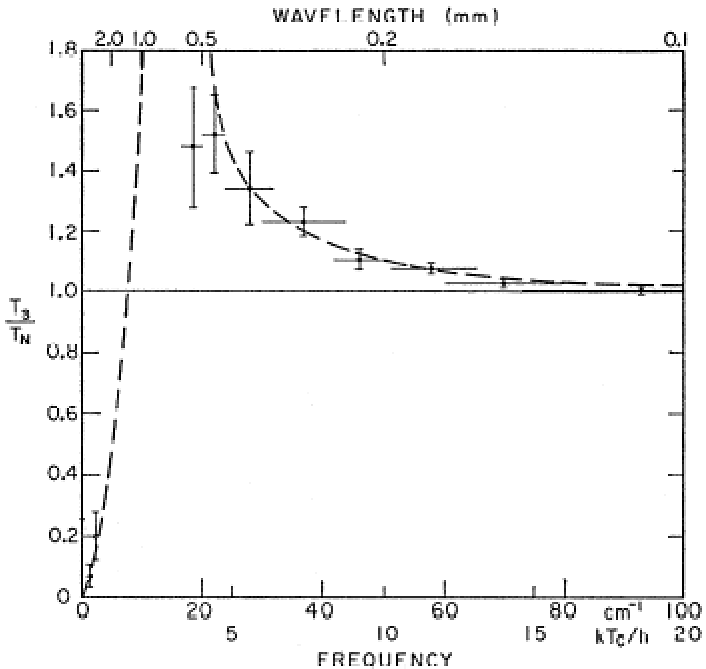

FIG. 1. Experimental transmission ratios of superconducting and normal states of a typical lead film (dc residual resistance 117 ohms; transmission in normal state $=\frac{1}{4}$) at $T/T_c = 0.67\pm0.03$. The frequency uncertainty on each infrared point is the half-power width of the continuous spectrum used. The vertical error limits on these points are derived statistically from the data. The dashed curve is one proposed for $T=0$ and an energy gap of $3kT_c$, as described in the following Letter.

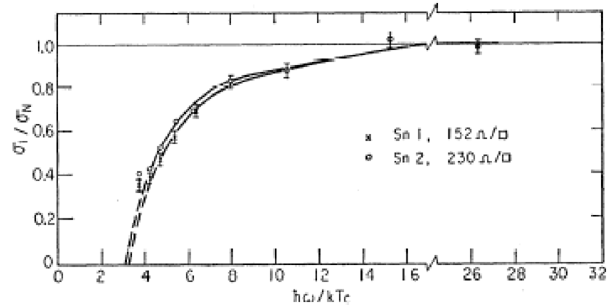

FIG. 8. Frequency dependence of σ_1/σ_N for Sn1 and Sn2.

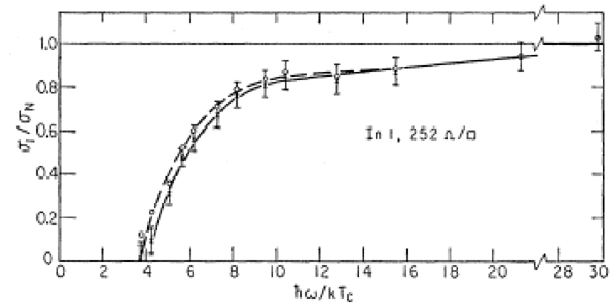

FIG. 9. Frequency dependence of σ_1/σ_N for In1. The solid curve is calculated using the measured film resistance, the broken curve using the calculated value. (See text.)

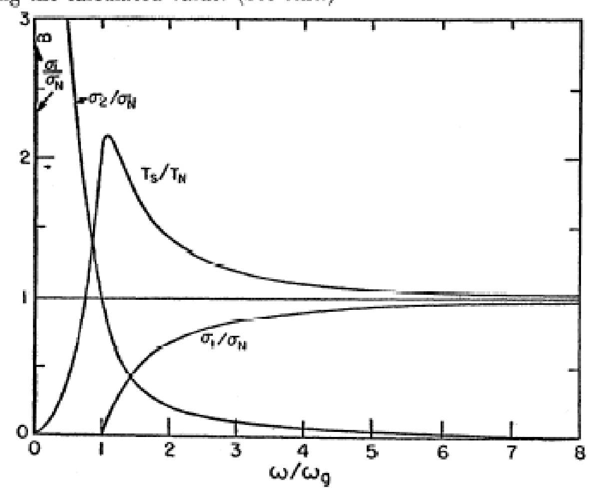

FIG. 10. Frequency dependence of σ_1/σ_N, σ_2/σ_N, and T_S/T_N according to the calculation of Mattis and Bardeen. The transmission curve is for a film resistance $377/(n+1)$ ohms per square, where n is the refractive index of the substrate.

R. E. Glover and M. Tinkham, Phys. Rev. **104**, 844 (1956)

$\frac{\sigma_1}{\sigma_n}$

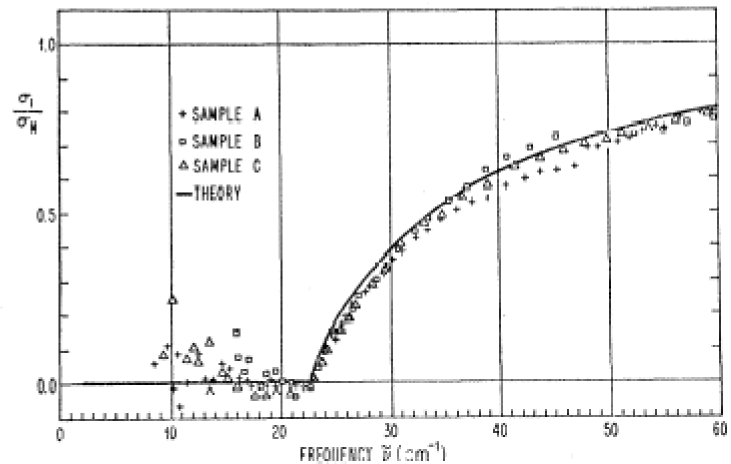

FIG. 3. Results of measurements of the real part of the normalized conductivity of three thin lead films at 2°K, compared with Mattis–Bardeen theory with gap frequency fitted to 22.5 cm^{-1}. To reduce the clutter in the figure, only about one fourth as many points are shown as were taken and recorded in Ref. 7. The points shown are selected typical points above the gap and local averages below the gap.

$\frac{\sigma_1}{\sigma_n}$

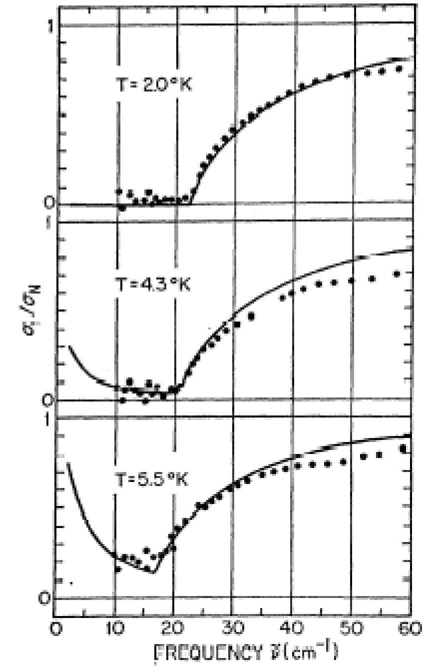

FIG. 4. Temperature and frequency dependence of normalized conductivity σ_1/σ_N in a thin superconducting lead film (sample C), compared with predictions of Mattis–Bardeen theory (calculated with the assistance of a program supplied by Harris), shown as solid curve. The gap frequency was fitted only for the low-temperature limit. The number of data points shown has been reduced as in Fig. 3.

L. H. Palmer and M. Tinkham, Phys. Rev. **165**, 588 (1968)

Absence of Case II Coherence Effects in Cuprates

$1/T_1$

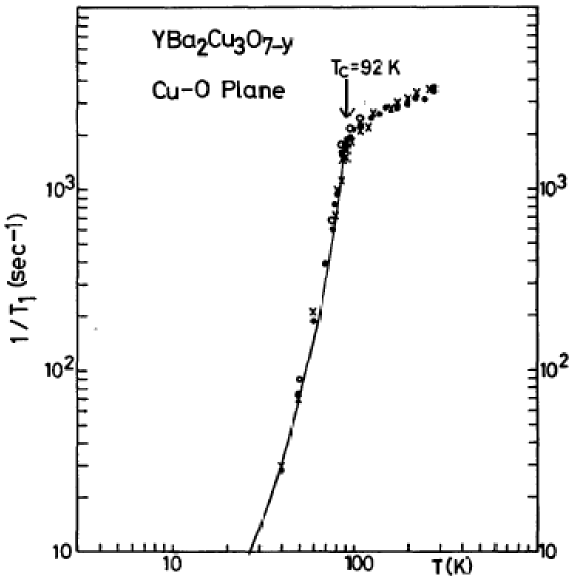

Y. Kitaoka, *et al*., J. Phys. Soc. Japan **57**, 30 (1988)

Reasons for absence of coherence effects in high-T_c cuprates

Gap anisotropy

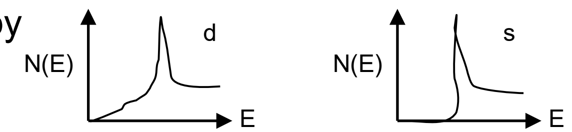

Spin fluctuations (not QPs) dominate spin relaxation

Clean limit electrodynamics (suppresses "coherence peak")

The absence of "coherence effects" does not rule out a BCS-like description of the cuprates

$$\frac{\sigma_1}{\sigma_n}$$

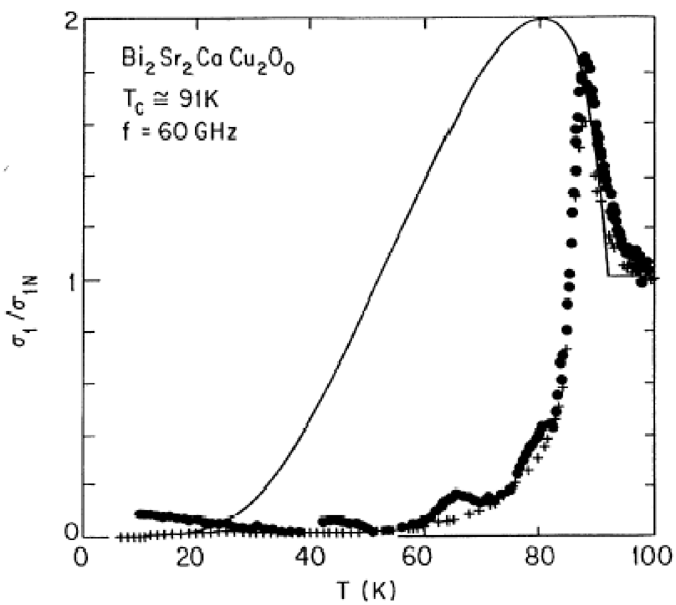

K. Holczer, *et al*., Phys. Rev. Lett. **67**, 152 (1991)